

**Manuscript version: Author's Accepted Manuscript**

The version presented in WRAP is the author's accepted manuscript and may differ from the published version or Version of Record.

**Persistent WRAP URL:**

<http://wrap.warwick.ac.uk/146555>

**How to cite:**

Please refer to published version for the most recent bibliographic citation information. If a published version is known of, the repository item page linked to above, will contain details on accessing it.

**Copyright and reuse:**

The Warwick Research Archive Portal (WRAP) makes this work by researchers of the University of Warwick available open access under the following conditions.

© 2020 Elsevier. Licensed under the Creative Commons Attribution-NonCommercial-NoDerivatives 4.0 International <http://creativecommons.org/licenses/by-nc-nd/4.0/>.



**Publisher's statement:**

Please refer to the repository item page, publisher's statement section, for further information.

For more information, please contact the WRAP Team at: [wrap@warwick.ac.uk](mailto:wrap@warwick.ac.uk).

# Data driven learning model predictive control of offshore wind farm

Xiuxing Yin <sup>a</sup> and Xiaowei Zhao <sup>b,\*</sup>

<sup>a</sup> School of Mechanical and Electrical Engineering, Guilin University of Electronic Technology, 541004 Guilin, P.R. China

<sup>b</sup> School of Engineering, The University of Warwick, Coventry CV4 7AL, U.K.

\*Corresponding author: xiaowei.zhao@warwick.ac.uk

## Abstract

This paper presents a data-driven control approach for maximizing the total power generation of the offshore wind farm by using a recently developed learning model predictive control (LMPC) algorithm. The control is designed by coordinating yaw angle control actions of wind turbines to mitigate the wake interactions among the turbines for increasing the total farm power production, which is termed as wake redirection. This paper mainly focuses on designing the architecture and methodology of the LMPC for wind farm, including a unified wind turbine wake interaction model, the LMPC for minimizing an iteration cost function, the recursive feasibility, stability and convergence analysis. Extensive comparative studies are conducted to verify the performance of the LMPC in comparison with the existing model predictive control (MPC) method under the same wind speed conditions. The results show that the wind farm yields up to 15% more power production by using the LMPC than the conventional MPC.

**Keywords:** Wind farm; Learning model predictive control; Wake interaction; Wake redirection; FLORIS wind farm model.

## I. INTRODUCTION

Wind energy is increasingly becoming one of the most popular renewable energy sources around the world and will fulfill one third of the world's electricity need by 2050 [1]. The global investment share of offshore wind in the wind energy has risen steadily from 10% in 2013 to 25% in 2016 [2]. An offshore wind farm is a cluster of wind turbines that are collected together in each other's proximity to reduce maintenance costs. However, wind turbines in an offshore wind farm experience up to 40% power losses due to the aerodynamic wake interaction [3] which is generated from the upwind turbines and therefore can lower the wind power production of downwind turbines inside the wake region. The wake interaction is generally characterized by increased turbulence and reduced wind flow velocity, and is highly dependent on the number of wind turbines and atmospheric conditions including wind speed, wind direction, and turbine control settings such as blade pitch angles, generator torques, and yaw angles [4].

The challenges in mitigating complex wake effects in offshore wind farms and therefore increasing wind farm power production have motivated the development of a wide variety of approaches in the wind energy research area. One approach is to carefully optimize the wind farm layout by allowing enough space between turbine locations in the design phase. However, this optimization may be limited due to the stochastic nature of continuously varying wind conditions. Besides the design optimization, another possible approach, is to down regulate individual turbines from their peak power points in order to maximize the wind farm power production as a whole. However, this turbine downregulation method maybe highly suboptimal due to the poor understanding and

31 mitigation of turbine-wake interactions in an offshore wind farm. Therefore, the efforts should be made towards joint setting of  
32 control variables or coordinating control settings of individual wind turbines for reducing power losses due to wake interactions  
33 and hence maximizing the total wind farm power generation. Actually, the axial induction factors and the yaw-offset angles of  
34 individual wind turbines can be employed as the control variables to mitigate the wake effects. The axial induction factor can be  
35 generally regulated by adjusting the generator torque and the blade pitch angle in a wind turbine. The yaw-offset angle, defined as  
36 the misalignment angle between the wind rotor and the wind direction, can be intentionally and intelligently yawed out of the wind  
37 direction to deflect the wake trajectory away from downwind turbines, thereby increasing the wind power productions of  
38 downstream wind turbines. The method of adjusting the yaw-offset angles can be generally termed as the *wake redirection control*.  
39 Although the control of both the induction factors and the yaw-offset angles can be conducted simultaneously, the wake redirection  
40 control is easy to implement and has much greater potential in maximizing the total wind farm power production.

41 Recently, the active regulation of induction factor and yaw angle for mitigating the wake interference and improving the total  
42 wind farm power production have been a hot topic and different control perspectives have been reported in the literature. For  
43 example, the gradient ascent algorithm [5], the game-theoretic search algorithm [6], the simultaneous perturbation stochastic  
44 approximation method [7], and the maximum power point tracking methods [8] have been proposed for maximizing the wind farm  
45 power production, and some of them have been evaluated by using large eddy simulation model such as the Parallelized Large-  
46 eddy simulation Model (PALM) [9]. In [10], an optimization approach was employed to determine the optimal control actions for  
47 maximizing the wind farm power based on the sequential quadratic programming. However, the optimization was designed based  
48 on analytical wind farm power functions with simplified wake models, which cannot precisely reflect the wind farm conditions. In  
49 [11], the optimal turbine yaw-offset angles were derived by using a parametric wind farm power function that was constructed  
50 from a high-fidelity Computational Fluid Dynamics (CFD) simulation. However, a large amount of wind turbine parameters and  
51 environmental variables need to be specified in the CFD model.

52 In [12], the feasibility of using the Bayesian Ascent (BA) algorithm for determining the coordinated optimal control actions for  
53 a wind farm was evaluated with different number of wind turbines and time-varying wind conditions. However, this parametric  
54 study was based on analytical wind farm power function, and the used BA algorithm may incur an excessive number of iterations  
55 when scaling up to optimize a large number of wind turbines. In [13], the Bayesian optimization (BO) was used to find the optimal  
56 inputs for a wind farm in the context of exploration and exploitation based sequential decision-making. However, the BO needs  
57 the prior description of the target function using Gaussian process and requires a large amount of data points to reach the optimal  
58 operational conditions. In addition, the BO may not perform well with noisy measurement data and cannot be used in real-time  
59 control applications due to constraints in the (conventional) sampling strategies in BO. In [14], the game theory and cooperative  
60 control were used to optimize wind farm energy production based on the framework of enmeshed decision making where individual

61 turbines represent the decision makers. In [15], a constrained time efficient closed-loop wind farm control approach was introduced  
62 and evaluated in a parameter-varying realistic wind farm flow model. In [16], two decentralized discrete adaptive filtering  
63 algorithms were proposed to optimize the total wind farm power output with only limited information sharing among neighbor  
64 turbines and without using the wind farm power generation model. The fast convergence to the optimal total power generation and  
65 high efficiency of the algorithms were demonstrated by simulation. In [17], the influence of optimal control parameters on wind  
66 farm optimization was quantified and the simulation results indicated that up to 21% gain in wind farm power production could be  
67 achieved by using optimization. In [18], an optimization under uncertainty (OUU) method was formulated to find the optimal wake  
68 redirection strategy in the presence of yaw angle uncertainty. A utility-scale two-turbine test case was used to demonstrate the  
69 method, and the results indicated that the OUU solution improved the overall annual average energy by 0.2% and produced fewer  
70 extreme yaw situations than the deterministic solution when considering the realistic uncertainty.

71 In [19], a constrained model predictive control (MPC) was proposed for maximizing the total wind farm power production by  
72 using a two-dimensional dynamic wind farm model to predict wake interactions. The wind turbine axial induction factors were  
73 used as control inputs and an adjoint approach was utilized to compute the optimal induction factors. The control effectiveness of  
74 the approach was demonstrated based on a  $2 \times 3$  wind farm. In [20], a control algorithm was proposed to maximize the wind farm  
75 power reserve by distributing the power contribution of each wind turbine. The evaluation of the algorithm was conducted by  
76 simulations of 12 wind turbines. In [21], a closed-loop receding horizon controller was proposed based on a time-varying one-  
77 dimensional wake model to provide secondary frequency regulation in a wind farm. The controller was designed by using wind  
78 speed measurements of each wind turbine as feedback and was then tested in large eddy simulations of an 84-turbine wind farm.  
79 In [22], a distributed MPC scheme was proposed and solved by distributed optimization at every time step. Two MPC versions  
80 respectively with hard constraint and soft constraint of the farm-wide power output were implemented and compared. An  
81 alternating direction method of multipliers and a dual decomposition scheme were compared in the distributed optimization. Four  
82 exemplary scenarios was used to test the performance of the distributed MPC controller and the distributed optimization methods.  
83 The results implied that the use of the distributed MPC in wind farms is viable. In [23], a distributed MPC was presented for the  
84 optimal active power control of a wind farm that was equipped with fast and short-term energy storage system. A gradient method  
85 via dual decomposition was used to implement the distributed MPC. Case studies were performed to evaluate the effectiveness of  
86 the distributed MPC whose efficiency is independent from the wind farm size.

87 This paper aims to develop a new wake redirection control strategy based on the recent learning model predictive control  
88 (LMPC) approach [25], [26] to improve the performance of the traditional MPC in maximizing the total offshore wind farm power  
89 production. The LMPC is a data driven approach that can iteratively improve the wind farm power production and minimize the  
90 control action burden by learning the input trajectories and state cost from previous iterations. The LMPC is designed and

91 implemented iteratively by solving a finite-time constrained optimization problem that can minimize a finite-time predicted cost  
 92 while handling state and inputs constraints. The LMPC scheme is reference-free and is able to improve its performance (in  
 93 comparison with MPC) by learning from previous iterations. A convex safe set and a terminal cost function, learnt from previous  
 94 iterations, are used in the LMPC to allow for the consideration of the long term planning and can guarantee the stability, recursive  
 95 feasibility and performance improvement of the control object. Moreover, the converged steady-state trajectory is locally optimal  
 96 for an approximation of the infinite horizon control problem.

97 The solution of the LMPC in the wind farm control is a sequence of optimized joint yaw angles that can be used to minimize  
 98 the cost function while satisfying the recursive stability and convergence performance. By using extensive co-calculations based  
 99 on the data-driven FLORIS (FLOW Redirection and Induction in Steady-state) tool developed by NREL (National Renewable  
 100 Energy Laboratory) and the MATLAB software, greatly improved performance of the LMPC method in maximizing the offshore  
 101 wind farm power capture has been demonstrated based on a comparison with the existing MPC method. The former results in up  
 102 to 15% more power production than the latter.

103 The rest of the paper is organized as follows: in section II, the wind farm model and the control problem are formulated. In  
 104 section III, the LMPC design and related stability proof are presented. In section IV, the validations and discussions of the  
 105 developed LMPC wind farm control strategy are presented, based on the FLORIS model. Section V includes the conclusion of this  
 106 paper.

## 107 II. WIND FARM MODEL AND PROBLEM FORMULATION

108 In order to derive and implement the LMPC for a wind farm, it is necessary to formulate a wind farm model based on the wind  
 109 turbine wake model and wake interaction model among the turbines. Also, it is essential to study the effects of yaw offset angles  
 110 on the wind farm power production to formulate the predictive control problem.

### 111 A. Wind Turbine Wake Model

112 The commonly used and computationally efficient wind turbine wake model is the Jensen model (or the Park wake model) [24]  
 113 which assumes that the wind velocity in a wake is uniform and expands proportionally to the axial downstream distance from the  
 114 turbine rotor. As shown in Fig. 1, for a turbine  $i$  within a wind farm, the wake behind this turbine can be divided into three separate  
 115 regions, i. e. near wake ( $q = 1$ ), far wake ( $q = 2$ ), and mixing regions ( $q = 3$ ), while each region has a diameter  $D_{w,i,q}$ , ( $q=1, 2, 3$ )  
 116 [11]. The near-wake region is influenced by the local chord Reynolds number and the turbine tip speed ratio. In the far wake region,  
 117 the wind velocity deficits with the distance from the turbine rotor. In the mixing region, due to the turbulence-induced mixing, the  
 118 wind velocity will gradually recover to the free-stream velocity.

119 The wind velocity behind a turbine  $i$  is modeled as

$$V_{w,i}(x, y) = V_\infty [1 - 2a_i c_i(x, y)] \quad (1)$$

where  $V_\infty$  is the free-stream inflow wind velocity,  $a_i$  is the axial induction factor of the turbine  $i$  that can be defined as the relative amount of velocity drop at the turbine rotor with respect to the inflow velocity,  $c_i(x, y)$  is a piecewise wake decay coefficient that can be defined as follows

$$c_i(x, y) = \begin{cases} c_{i,1}(x) & \text{when } |y - y_{w,i}(x)| \leq D_{w,i,1}(x)/2 \\ c_{i,2}(x) & \text{when } D_{w,i,1}(x)/2 < |y - y_{w,i}(x)| \leq D_{w,i,2}(x)/2 \\ c_{i,3}(x) & \text{when } D_{w,i,2}(x)/2 < |y - y_{w,i}(x)| \leq D_{w,i,3}(x)/2 \\ 0 & \text{when } |y - y_{w,i}(x)| > D_{w,i,3}(x)/2 \end{cases} \quad (2)$$

where  $c_{i,q}(x)$ ,  $q = 1, 2, 3$  is the local wake decay coefficient for each region,  $y_{w,i}(x)$  is the position of the wake centerline when  $x > X_i$ .

The local wake decay coefficient  $c_{i,q}(x)$ ,  $q = 1, 2, 3$  is

$$c_{i,q}(x) = \left[ \frac{D_i}{D_i + 2k_e m_{v,q}(u_i)(x - X_i)} \right]^2, q = 1, 2, 3 \quad (3)$$

where  $D_i$  is the rotor diameter of the turbine  $i$ ,  $k_e$  and  $m_{v,q}(u_i)$  are the wake expansion coefficients,  $u_i(t)$  is the control input for the turbine, which is the yaw angle of the turbine in the wake redirection control.

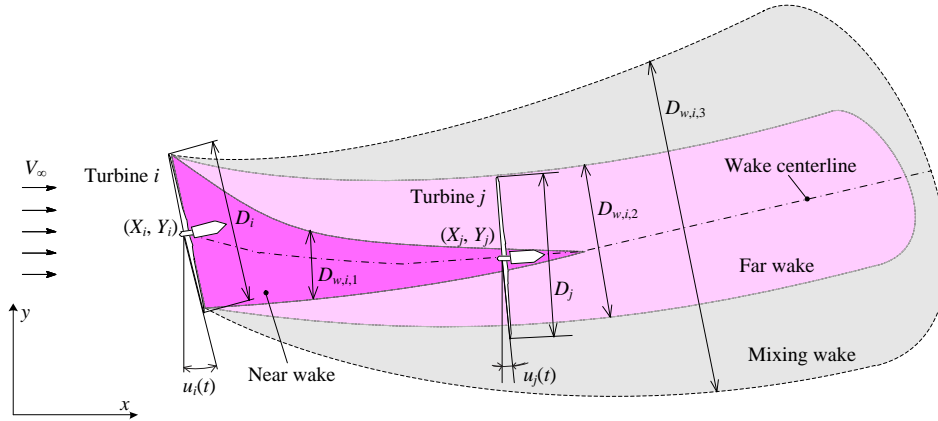


Fig. 1 Schematic of the wake regions behind the turbine  $i$

The coefficient  $m_{v,q}(u_i)$  is directly related to the yaw angle offset via the following relationship

$$m_{v,q}(u_i) = \frac{M_{v,q}}{\cos(a_v + b_v u_i(t))}, q = 1, 2, 3 \quad (4)$$

where  $M_{v,q}$ ,  $a_v$ , and  $b_v$  are constant.

The diameters of the wake regions  $D_{w,i,q}$  in (2) is

$$D_{w,i,q}(x) = \max(D_i + 2k_e m_{e,q}(x - X_i), 0) \quad (5)$$

138 where the scaling parameter  $m_{e,q}, q = 1, 2, 3$  denotes the wake expansion rate of the three regions.

139 The position of the wake centerline is determined by combining the yaw-induced and rotation-induced wake lateral offsets with  
 140 respect to the hub coordinate of the turbine  $i$  as follows

$$141 \begin{cases} y_{w,i}(x) = Y_i + \delta y_{w,rot,i}(x) + \delta y_{w,yaw,i}(x, u_i, a_i) \\ \delta y_{w,rot,i}(x) = a_d + b_d(x - X_i) \\ \delta y_{w,yaw,i}(x, u_i, a_i) = \int_0^{x-X_i} \tan(\xi_i) dx \\ \xi_i = \frac{2a_i(1-a_i)\cos^2(u_i)\sin(u_i)}{\left(1 + 2k_d \frac{x-X_i}{D_i}\right)^2} \end{cases} \quad (6)$$

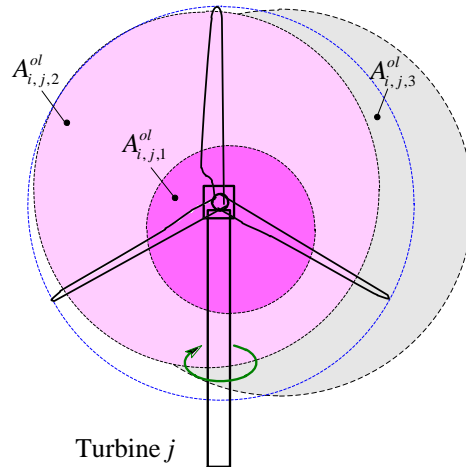
142 where  $\delta y_{w,rot,i}(x)$  and  $\delta y_{w,yaw,i}(x, u_i, a_i)$  are respectively the rotation and yaw induced offsets of the wake centerline position. The  
 143 coefficients  $a_d$ ,  $b_d$  and  $k_d$  are constant in determining the centerline position.

#### 144 B. The Wake Interaction Model

145 Considering a turbine  $j$  in the wake regions of the turbine  $i$ , the overlapping areas between the turbine rotor and the three wake  
 146 regions is shown in Fig. 2. Then, the effective inflow wind velocity of the turbine  $j$  is readily calculated by weighting the wake  
 147 regions by the overlapping areas with the turbine rotor. Therefore, the effective inflow speed  $V_j$  of the downstream turbine  $j$  takes  
 148 the following form [11]

$$149 V_j = V_\infty \left( 1 - 2 \sqrt{\sum_{i \in \mathbb{N}; X_i < X_j} \left( a_i \sum_{q=1}^3 c_{i,q}(X_j) \min\left(\frac{A_{i,j,q}^{ol}}{A_j}, 1\right) \right)} \right) \quad (7)$$

150 where  $(X_j, Y_j)$  denotes the coordinate of the turbine  $j$ ,  $A_{i,j,q}^{ol}, q = 1, 2, 3$  is the overlapping areas of the three wake regions with the  
 151 turbine rotor,  $A_j$  is the turbine rotor area.



152

153

Fig. 2 Schematic of the overlapping areas of the turbine  $j$

154 As illustrated in (7), the inflow wind velocity of the turbine  $j$  is not only related to its own yaw angle, but also is influenced by  
 155 the yaw angle of the upstream turbine  $i$ , which clearly indicates that the inflow wind power of the downstream wind turbine  $j$  is  
 156 affected by the yaw angle control inputs of itself and the upstream turbines. Therefore, the changes of the operational conditions  
 157 of upstream turbines influence the inflow wind velocity of a downstream wind turbine through wake interactions, which therefore  
 158 influence the power extraction of downstream turbine. The wind velocity of upstream turbines that are located in the front of a  
 159 wind farm and that are not influenced by other turbines can be determined as  $V_j = V_\infty$ .

### 160 C. The Control Problem Formulation

161 For a large-scale wind farm with  $N$  wind turbines denoted by the set  $\aleph = \{1, 2, \dots, N\}$ , each wind turbine  $j$  is characterized by its  
 162 rotor diameter  $D_j$ , induction factor  $a_j$ , inflow wind velocity  $V_j(t)$  and yaw angle offset  $u_j(t)$ .

163 Based on the actuator disc theory, the power extracted from a single turbine  $j$  is equivalent to the amount of power extracted by  
 164 the rotor disc as follows [12]

$$165 \quad P_j(t) = \frac{\pi\rho D_j^2}{8} \left[ V_j(t) \cos(u_j(t)) \right]^3 C_{pj}(a_j, u_j(t)) \quad (8)$$

166 where  $P_j(t)$  is the power extracted from the turbine  $j$ ,  $\rho$  is the air density, and [16]

$$167 \quad C_{pj}(a_j, u_j) = 4a_j(1-a_j)^2 \cos(u_j(t))^2 \quad (9)$$

168 is the power coefficient of the turbine.

169 The total wind power extraction  $x(t)$  of the wind farm is an aggregation of the powers produced by all the wind turbines

$$170 \quad x(t) = \sum_{j=1}^N P_j(t) = \sum_{j=1}^N \frac{\pi\rho D_j^2}{8} \left[ V_j(t) \cos(u_j(t)) \right]^3 C_{pj}(a_j, u_j(t)) \quad (10)$$

171 In the case of wake redirection control, by assuming the constant induction factor  $a_j$  and the constant variation rate of the yaw  
 172 angle offset  $\dot{u}_j(t)$ , the time derivative of the wind farm power is determined based on (8)~(10) as follows

$$173 \quad \dot{x}(t) = \sum_{j=1}^N \frac{3\pi\rho D_j^2 a_j (1-a_j)^2 \left[ V_j(t) \cos(u_j(t)) \right]^2 \cos(u_j(t))^2 \left[ \dot{V}_j(t) \cos(u_j(t)) - \right.}{2 \left. \left[ V_j(t) \dot{u}_j(t) \sin(u_j(t)) \right]} \right. \quad (11)$$

$$- \sum_{j=1}^N \pi\rho D_j^2 a_j (1-a_j)^2 u_j(t) \left[ V_j(t) \cos(u_j(t)) \right]^3 \sin(u_j(t))^2 \dot{u}_j(t)$$

174 Therefore, by using a constant time interval  $\Delta t$  for the time differential operation in (11), the time derivative of the wind farm  
 175 power in (11) can be reasonably represented as

$$176 \quad \dot{x}(t) = \frac{x(t+\Delta t) - x(t)}{\Delta t} \Rightarrow x(t+\Delta t) = x(t) + \dot{x}(t)\Delta t \Rightarrow x(t+\Delta t) = f_p(x(t), u_j(t)), \forall j \in \aleph \quad (12)$$

177 By observing (9)-(12) and the wake model in (1)-(7), the wind farm power can be generally characterized by the function



178  $f_p(x(t), u_j(t))$  in (12) and is only directly related to the joint yaw angle offset of the turbines within the wind farm in the wake  
 179 redirection control case. Therefore, by properly regulating the joint yaw angles of the turbines, the state of the wind farm power  
 180 extraction can be varied accordingly, which forms the control problem of yaw angle redirection control in maximizing the wind  
 181 farm power generation.

182 In practice, the nonlinear function  $f_p(x(t), u_j(t))$  in (12) can be well parameterized and accurately represented by using the  
 183 FLORIS wind farm model with each wind turbine represented by the offshore 5 MW NREL wind turbine model. As a consequence,  
 184 with the power function being explicitly defined above, the LMPC scheme can be employed to solve the wind farm power  
 185 maximization problem.

### 186 III. THE LMPC FOR WIND FARM

187 In this section, the LMPC approach [25], [26] is explored for developing the wake redirection control to maximize the total wind  
 188 farm power production. The LMPC is designed and implemented iteratively by solving a finite-time constrained optimization  
 189 problem. The solution is a sequence of optimized joint yaw angles that can be used to minimize an iteration cost function of the  
 190 wind farm power generation. Then, the LMPC is proved to be recursively feasible and stable at each successive iteration, and the  
 191 iteration cost is guaranteed to be non-increasing at all time instants and iterations.

#### 192 A. The LMPC Design

193 The wind farm power maximization problem formulated in the above section is equivalent to the minimization of its reciprocal

$$194 \frac{1}{x(t + \Delta t)} \text{ or } \frac{1}{x(t)}.$$

195 In order to transform the continuous time domain wind farm state equation in (12) into the discrete time domain to facilitate the  
 196 LMPC design, the following variables are defined

$$197 \begin{cases} x_{t+1} = \frac{1}{x(t + \Delta t)}; \\ x_t = \frac{1}{x(t)}; \\ u_t = [u_1(t), \dots, u_j(t), \dots, u_N(t)] \\ \Delta t = 1. \end{cases} \quad (13)$$

198 where  $x_{t+1}$  and  $x_t$  denote the state variables at time instants  $t$  and  $t+1$ , respectively,  $u_t$  denotes the joint set of the yaw angles at  
 199 time instant  $t$ .

200 Based on (13), (12) can be transformed into the discrete time domain as follows

$$x_{t+1} = \frac{1}{x(t+\Delta t)} = \frac{1}{x(t) + \dot{x}(t)\Delta t} \Rightarrow x_{t+1} = \frac{\frac{1}{x(t)}}{1 + \frac{\dot{x}(t)}{x(t)}\Delta t} \Rightarrow x_{t+1} = \frac{x_t}{1 + \dot{x}(t)x_t} \quad (14)$$

Therefore, based on (10)-(14), the state equation of the wind farm is represented as

$$x_{t+1} = f(x_t, u_t) \quad (15)$$

where  $f(\cdot)$  represents the nonlinear relationship between the control input  $u_t$  and state variable  $x_{t+1}$ , and can be characterized by the function  $f_p(x(t), u_j(t))$  in (12) or represented by using the FLORIS wind farm model.

In general, the nonlinear function  $f(\cdot)$  is continuous at all time instants, and the state and inputs are subject to necessary constraints.

At the  $j$ th iteration of the LMPC task, the state trajectory and the associated control input sequence are

$$\begin{cases} \mathbf{x}^j = [x_0^j, \dots, x_t^j, \dots, x_{T^j}^j]; \\ \mathbf{u}^j = [u_0^j, \dots, u_t^j, \dots, u_{T^j-1}^j]. \end{cases} \quad (16)$$

where  $x_t^j$  and  $u_t^j$  denote the state trajectory and control input at the time instant  $t$  of the  $j$ th iteration,  $T^j$  is the time instant at which the control task is completed.

At each  $j$ th iteration, the state trajectory is assumed to start from the same initial state. Then, by using the stored data in (16), a convex safe set  $CS^j$  at the  $j$ th iteration can be constructed [25]. Thus,

$$CS^j = \text{Conv} \left( \bigcup_{i=0}^j \bigcup_{t=0}^{T^i} x_k^i \right) \quad (17)$$

Actually, the convex safe set  $CS^j$  can be defined as the convex hull of the union of the stored data as follows

$$CS^j = \left\{ x \in \mathbf{R} : \exists \lambda_k^i \geq 0, \sum_{i=0}^j \sum_{t=0}^{T^i} \lambda_k^i = 1, \sum_{i=0}^j \sum_{t=0}^{T^i} \lambda_k^i x_k^i = x \right\} \quad (18)$$

where  $\lambda_k^i$  denotes the Lagrange multiplier associated with each recorded data in the convex safe set.

Also, based on the stored data in (16), a continuous cost-to-go function can be defined as

$$Q_k^j = h(x_k^j, u_k^j) + Q_{k+1}^j \quad (19)$$

where  $Q_k^j$  is the cost-to-go function defined at the  $k$  time instant of the  $j$ th iteration. At the time instant  $T^j$  when the control task is completed, the cost to go function can be defined as

$$Q_{T^j}^j = h(x_{T^j}^j, 0), \forall j > 0 \quad (20)$$

For the wind farm control task, the cost function in (19) and (20) can be defined as

$$224 \quad h(x_k^j, u_k^j) = (x_k^j)^T Q x_k^j + (u_k^j)^T R u_k^j \quad (21)$$

225 where  $Q=10000$ ,  $R=I_N$  ( $I_N$  is a  $N \times N$  dimension identity matrix) are the constant coefficients, respectively.

226 Then, the Q-function to be optimized can be defined based on (19)-(21) as follows

$$227 \quad Q^{j,*}(x) = \min_{\lambda_k^i \in [0,1]} \sum_{i=0}^j \sum_{k=0}^{T^i} \lambda_k^i Q_k^i \quad (22)$$

$$\text{s.t.} \begin{cases} \sum_{i=0}^j \sum_{k=0}^{T^i} \lambda_k^i = 1 \\ \sum_{i=0}^j \sum_{k=0}^{T^i} \lambda_k^i x_k^i = x \end{cases}$$

228 The above Q-function defined in (22) can be used as the terminal cost in an infinite horizon optimal control problem. Therefore,  
229 the control problem defined in the section II-C can be equivalently transformed into the infinite horizon optimal control problem  
230 at each  $j$ th iteration as follows [26]

$$231 \quad J_{t \rightarrow t+n}^j(x_t^j) = \min_{U_t^j, \lambda^j} \left[ \sum_{k=t}^{t+n-1} h(x_{k/t}^j, u_{k/t}^j) + \sum_{i=0}^{j-1} \sum_{k=0}^{T^i} \lambda_k^i Q_k^i \right] \quad (23)$$

232 where  $n$  is the prediction time horizon.

233 The cost function defined in (23) includes a running cost  $\sum_{k=t}^{t+n-1} h(x_{k/t}^j, u_{k/t}^j)$  and the cost-to-go function  $\sum_{i=0}^{j-1} \sum_{k=0}^{T^i} \lambda_k^i Q_k^i$ . The control  
234 problem is also subject to the constraints of initial condition, dynamics constraint, state and input constraints that can be represented  
235 as

$$236 \quad \begin{cases} x_{t/t}^j = x_t^j; \\ x_{k+1/t}^j = f(x_{k/t}^j, u_{k/t}^j); \\ \sum_{i=0}^{j-1} \sum_{k=0}^{T^i} \lambda_k^i = 1, \lambda_k^i \geq 0; \\ \sum_{i=0}^{j-1} \sum_{k=0}^{T^i} \lambda_k^i x_k^i = x_{t+n/t}^j; \\ u_{\min} \leq u_{k/t}^j \leq u_{\max}, \forall k = t, \dots, t+n-1. \end{cases} \quad (24)$$

237 where  $u_{\min}$  and  $u_{\max}$  represent the upper and lower bounds on the yaw control inputs. The constraints defined in (24) also enforce  
238 the latest predicted state  $x_{t+n/t}^j$  into the convex hull of the recorded states.

239 By solving (23) and (24), the optimal control sequence of the yaw angle offset can be obtained at the time instant  $t$  of the  $j$ th  
240 iteration as follows

$$241 \quad U_t^{j,*} = [u_{t/t}^{j,*}, \dots, u_{t+n-1/t}^{j,*}] \quad (25)$$

242 Consequently, the optimal control input applied to the wind farm at the time instant  $t$  of the  $j$ th iteration is obtained as

$$243 \quad u_t = u_{t|t}^{j,*} \quad (26)$$

244 Then, the infinite horizon optimal control problem proceeds and is repeated at the time instant  $t + 1$  based on the optimal control  
245 signal in (26) and the new state variable  $x_{t+1|t+1} = x_{t+1}^j$  until the maximum iteration number is exceeded.

246 The above infinite horizon optimal control problem defined in (23) and (24) is generally difficult to solve by using the traditional  
247 semidefinite programming and linear matrix inequalities especially when considering that the FLORIS wind farm model is  
248 implicitly involved in the problem. The constraints defined by the FLORIS wind farm model cannot be explicitly described by  
249 linear equations and many nonlinear relationships actually exist in the optimization problem. Therefore, the commercial or non-  
250 commercial semidefinite programming (SDP) solvers cannot be used. Then, the genetic algorithm (GA) is used to find the global  
251 optimal solution of the control input  $u_{t|t}^{j,*}$  at time instant  $t$  of the  $j$ th iteration. As a derivative free and powerful optimization tool  
252 inspired by evolutionary biology, the GA is designed based on the natural selection mechanism that includes the operators of  
253 selection, crossover, mutation, and inversion in a population candidate [27]. After a sufficiently high number of generations and  
254 population evolutions, the GA is capable of the global optimal solution with a satisfactory fitness level. In order to eliminate the  
255 heavy computational burden in the GA, the GA parameters including the generation number, the population size and the tolerance  
256 constraint can be carefully chosen to save time.

### 257 B. The Recursive Feasibility and Stability

258 The recursive feasibility and stability of the LMPC controlled wind farm system can be proved based on the designed convex  
259 safe set and the cost-to-go function. Also, there exists an asymptotically stable equilibrium point for the closed loop system at  
260 every iteration  $j \geq 1$  [26].

261 Considering the system (15) controlled by the LMPC in (26) and state update in (15), one obtains

$$262 \quad x_{t+1|t}^{*,j} = x_{t+1}^j \quad (27)$$

263 Given the related optimal input sequence and the optimal trajectory obtained by using (23) and (24), the cost function is obtained  
264 as

$$265 \quad J_{0 \rightarrow n}^j(x_{t+1|t}^{*,j}) = J_{0 \rightarrow n}^j(x_{t+1}^j) \quad (28)$$

266 Therefore, by defining  $Q^{j-1}(x_{t+n|t}^j) = \sum_{i=0}^{j-1} \sum_{k=0}^{T^i} \lambda_k^i Q_k^i$  and based on (27) and (28), the optimal cost can be used as a Lyapunov function

267 as follows

$$268 \quad \begin{aligned} J_{0 \rightarrow n}^j(x_t^j) &= \min_{U_t^j, \mathcal{U}_t^j} \left[ \sum_{k=0}^{n-1} h(x_{k|t}^j, u_{k|t}^j) + Q^{j-1}(x_{n|t}^j) \right] = h(x_{t|t}^{j,*}, u_{t|t}^{j,*}) + \sum_{k=1}^{n-1} h(x_{t+k|t}^{j,*}, u_{t+k|t}^{j,*}) + Q^{j-1}(x_{t+n|t}^{j,*}) \\ &= h(x_{t|t}^{j,*}, u_{t|t}^{j,*}) + \sum_{k=1}^{n-1} h(x_{t+k|t}^{j,*}, u_{t+k|t}^{j,*}) + h(x_t^{j,*}, u_t^{j,*}) + Q^{j-1}(x_{t+1}^{j,*}) \geq h(x_{t|t}^{j,*}, u_{t|t}^{j,*}) + J_{0 \rightarrow n}^j(x_{t+1|t}^{*,j}) \end{aligned} \quad (29)$$

269 where  $(i^*, t^*)$  in (29) is defined as

$$270 \quad (i^*, t^*) = \arg \min J_{0 \rightarrow \infty}^i(x_t^i), \forall x \in CS^i \quad (30)$$

271 Therefore,

$$272 \quad J_{0 \rightarrow n}^j(x_{t+1/t}^{j,*}) - J_{0 \rightarrow n}^j(x_t^j) \leq -h(x_{t/t}^{j,*}, u_{t/t}^{j,*}) < 0 \quad (31)$$

273 Due to the positive definitiveness of  $h(\cdot)$  in (21) and the continuity of  $J_{0 \rightarrow n}^j(\cdot)$ , it is obvious that the cost function in (31) is non-  
274 increasing along the closed loop trajectory and will reach an asymptotically stable point when  $t \rightarrow \infty$ .

### 275 C. The Convergence Analysis

276 The convergence property of the LMPC controlled wind farm can be analyzed based on the proof of the recursive feasibility  
277 and stability in section III-B. The cost defined in (23) will be non-increasing along the closed loop LMPC controlled wind farm  
278 system and will converges to a steady state trajectory  $x^\infty$  when time  $t \rightarrow \infty$  and the iteration  $j \rightarrow \infty$ . Then, the steady state yaw angle  
279 control input will be  $u^\infty = \lim_{j \rightarrow \infty} u^j$  which is the global optimal solution for the infinite horizon optimal control problem in (23)  
280 and (24).

281 The interested readers can refer to [28] for more details about the convergence analysis of the LMPC.

## 282 IV. VALIDATIONS AND DISCUSSIONS

283 In order to investigate and ascertain the efficiency and effectiveness of the LMPC designed for wake redirection control,  
284 computational experiments are conducted by using the NREL FLORIS tool and the MATLAB software. The experiments have  
285 been conducted under eleven different scenarios with different freestream wind speed inputs. A traditional MPC has been designed  
286 for comparison.

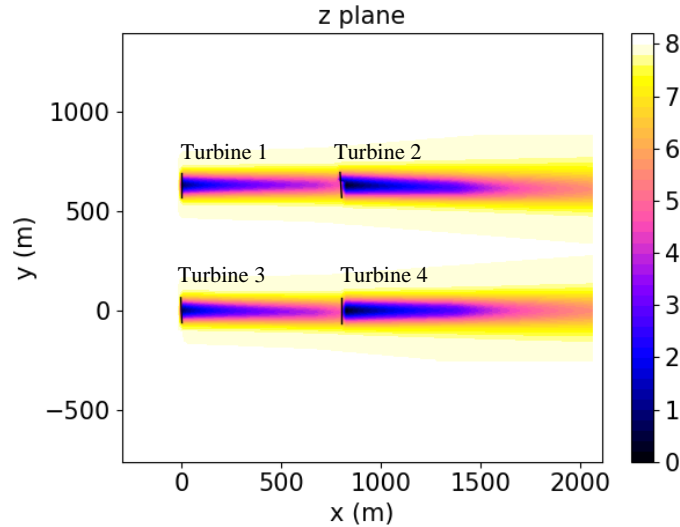
### 287 A. Computational Experiments

288 The computational experiments are carried out based on the co-calculations of MATLAB and the FLORIS tool when the inflow  
289 freestream wind speeds vary from 6 m/s to 11 m/s.

290 The FLORIS wind farm model is written in Python language and is designed to provide a controls-oriented and computationally  
291 inexpensive tool that models the turbine interactions and the steady-state wake characteristics in a wind farm. The FLORIS model  
292 is designed based on the Jensen model and the wake deflection by Jiménez et al., and hence is sufficiently fast to perform wake  
293 redirection control while retaining enough accuracy [29], [30]. The NREL 5 MW offshore wind turbine model with the rated wind  
294 speed of 12 m/s has been adopted in the FLORIS tool and the turbine yaw angles are bounded from  $0^\circ$  to  $15^\circ$ .

295 As shown in Fig. 3, the simulated wind farm consists of four wind turbines aligned in two rows with 800 m spacing in the  
296 downwind direction and 630 m spacing in the crosswind direction. The freestream wind speed comes from the front-left with the

297 direction of  $270^\circ$ , and turbines 1 and 3 are in the upstream direction while the turbine 2 and 4 are in the downstream wind direction.  
 298 The four turbines can interact fully through the wakes of the upstream turbines and therefore represent the realistic scenario for  
 299 wake redirection control. The incoming freestream wind speed varies from 6 m/s to 11 m/s and has the turbulence intensity of 5%  
 300 at the hub height, which represents the below-rated wind speed condition for the wind farm power optimization.



301  
 302 Fig. 3 The FLORIS wind turbine layout and wind speed distribution

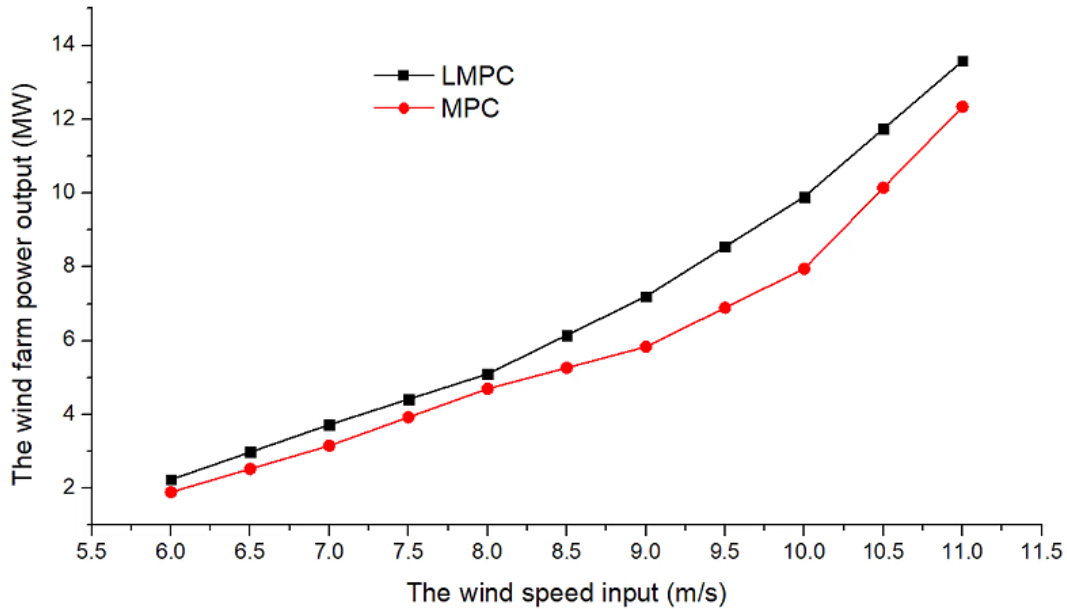
303 The LMPC algorithm has been designed and implemented in the MATLAB which calls the FLORIS tool by using the function  
 304 “*py.importlib.import\_module*” while the FLORIS tool defines an objective function with the turbine yaw angle vector as input and  
 305 the total wind farm power as output.

306 The genetic optimization tool (*gatool*) in the MATLAB has been used to solve the optimal control problem defined in (23) and  
 307 (24) for the LMPC implementation. The parameters of the genetic optimization have been carefully chosen in the “*gaoptimset*”  
 308 such that the LMPC problem can be solved efficiently with enough accuracy. For example, the number of generations has been set  
 309 as 30, the number of population size has been set as 50, and the operation parameters for crossover and mutation can be set as 0.6  
 310 and 0.2, respectively. The *gatool* calls the FLORIS tool for objective function evaluations at each time step with turbine yaw  
 311 settings as input and the calculated total wind farm power from the FLORIS tool as output. Other key parameters for the LMPC  
 312 have been set as: the controller horizon is 3 while the iteration number is 5. In order to further verify the effectiveness of the LMPC,  
 313 a traditional MPC has been designed for comparison.

### 314 B. Results and Analysis

315 As shown in Fig. 4, the total wind farm power increases with the increasing incoming wind speed from 6 m/s to 11 m/s with 0.5  
 316 m/s interval. It is obvious that the designed LMPC produces more power than the traditional MPC in the whole wind speed range.  
 317 At 6 m/s, LMPC increases the power capture by around 7.8% compared with the conventional MPC via the optimal turbine yaw  
 318 angle settings. This increase becomes more significant in the high-speed range of the wind and it reaches around 15% at 11 m/s.

319 The increase may be attributed to the fact that the LMPC can be used to find the optimal partial-wake operational point (through  
 320 iterative learning) where the wake-induced power losses are reduced due to less wake interactions among wind turbines. The results  
 321 also indicate that the LMPC method may be more suitable for the case of higher inflow wind speed.

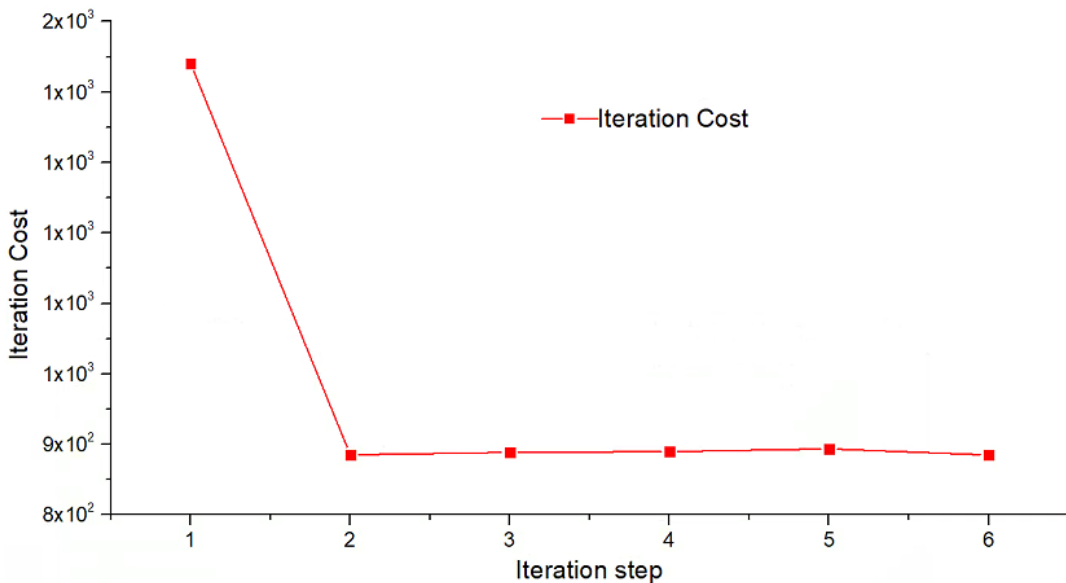


322

Fig. 4 The total wind farm power generations by using the two control algorithms

323

324 Fig. 5 demonstrates the evolution of the iteration cost of the LMPC under the incoming freestream wind speed of 8 m/s, which  
 325 is the typical result of all the wind speed scenarios. As shown in this figure, the iteration cost decreases almost monotonically with  
 326 the iterations and reaches the steady value of 858.2 in two iterations. This result demonstrates the recursive stability and  
 327 convergence of the LMPC, as mentioned in the sections III-B and C.



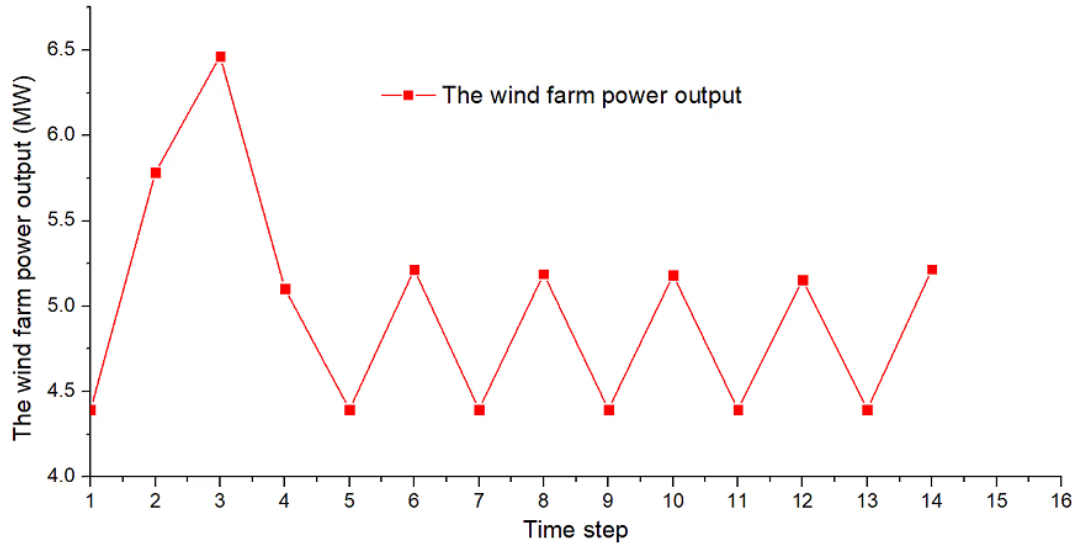
328

Fig. 5 The evolution of the iteration cost of the LMPC under the incoming freestream wind speed of 8 m/s

329

330 Fig. 6 illustrates the LMPC of wind farm energy extraction with the evolution of the total wind farm power production over the

331 prediction horizon at wind speed of 8 m/s. As shown in this figure, the total wind farm power evolves from 6.5 MW to 5.2 MW  
 332 with the decreasing iteration cost in Fig. 5. Although the 6.5 MW wind farm power is greater than the converged value of 5.2 MW,  
 333 its iteration cost involving the yaw angle actions is higher than the case at 5.2 MW as shown in Fig 6. It is clear that the LMPC  
 334 can be used to achieve a good trade-off between the control action cost and the optimal wind farm generation via executing several  
 335 trial expenses as shown in Fig. 6.



336

337 Fig. 6 The total wind farm power generation using the LMPC under the wind speed input of 8 m/s

338

338 Fig. 7 depicts the calculated time series of the optimal yaw angle settings in the four-turbine example at freestream wind speed  
 339  $V_\infty=8$  m/s. As shown in the figure, the trajectories of the yaw angles of the wind turbines 1, 2, 3 and 4 respectively evolve to the  
 340 optimal and steady values of  $15^\circ$ ,  $0.2238^\circ$ ,  $14.83^\circ$  and  $3.4697^\circ$  after the time step 5, which further demonstrates the stability and  
 341 convergence properties of the LMPC in section III. The yaw angles for front wind turbine 1 and 3 are set around the maximum  
 342 value of  $15^\circ$  so that their blades can be yawed out of the incoming wind and more wind energy can be captured by wind turbine 2  
 343 and 4 that have very small yaw angles. In this case, the total wind farm power output can be improved. The fluctuations of the  
 344 turbine yaw angles after the time step 5 may be caused by the self-similar Gaussian model in the new version FLORIS model,  
 345 which may have an impact on the total wind farm power output. Despite this, the converged values of the yaw angle settings are  
 346 required to sufficiently minimize the iteration cost function defined in (23) for the wind farm in a desirable manner in particularly  
 347 for wind farm system with fast dynamics.

348



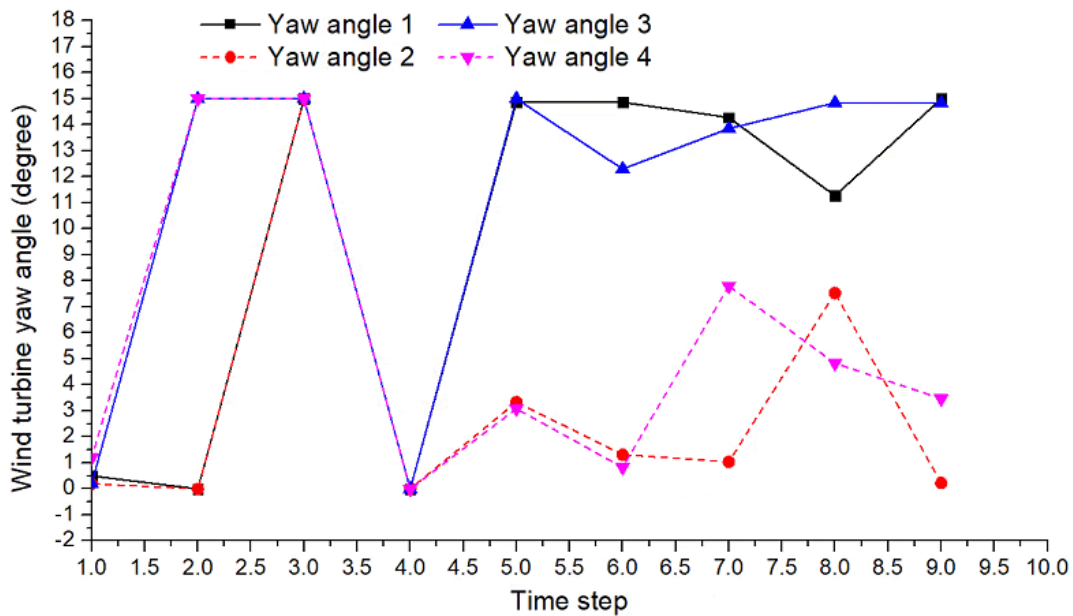


Fig. 7 The wind turbine yaw angles in the LMPC under the wind speed input of 8 m/s

## V. CONCLUSIONS

The data-driven LMPC has been proposed for increasing the total wind farm power production of offshore wind farm over a prediction horizon by iteratively executing the yaw angle control actions when considering the aerodynamic wake interactions among wind turbines. The LMPC can ensure the desired closed-loop control performance and improve execution efficiency simultaneously by learning from previous iterations. The detailed dynamic wake model and wake interaction model in a wind farm have been presented. The design details have been presented by recursively constructing the convex safe set and a terminal cost function for guaranteeing the control performance at each iteration. The convergence and global stability of the LMPC have also been proved. The effectiveness of the LMPC approach has been validated based on the co-calculations of the NREL FLORIS tool and the MATLAB. The results demonstrated that the LMPC converged fast to the optimal control set points of the yaw angles. In comparison to the conventional MPC, the wind farm yielded up to 15% more power production by using the LMPC.

We mention that the FLORIS model is a control-oriented steady-state wake model, which only provides information for the wake at a given wind condition. Therefore, the results in the work can be further improved by using dynamic CFD simulation tools like PALM or SOWFA. In the future work, we will investigate how to implement the control by using these dynamic CFD simulation tools for a large-scale wind farm.

## VI. ACKNOWLEDGEMENT

This work was funded by the UK Engineering and Physical Sciences Research Council under grant EP/R007470/1.

## REFERENCES

- 367
- 368 [1] <https://www.nationalgeographic.com/environment/global-warming/wind-power/>
- 369 [2] [https://www.irena.org/-/media/Files/IRENA/Agency/Publication/2018/Jan/IRENA\\_Global\\_Landscape\\_RE\\_finance\\_2018.pdf](https://www.irena.org/-/media/Files/IRENA/Agency/Publication/2018/Jan/IRENA_Global_Landscape_RE_finance_2018.pdf).
- 370 [3] Goit J, Munters W, Meyers J. Optimal coordinated control of power extraction in LES of a wind farm with entrance effects. *Energies*, 2016, 9(1): 29.
- 371 [4] Adaramola M S, Krogstad P Å. Experimental investigation of wake effects on wind turbine performance. *Renewable Energy*, 2011, 36(8): 2078-2086.
- 372 [5] Gebraad P M O, van Dam F C, van Wingerden J W. A model-free distributed approach for wind plant control. 2013 American Control Conference. IEEE, 2013:
- 373 628-633.
- 374 [6] Marden J R, Ruben S D, Pao L Y. A model-free approach to wind farm control using game theoretic methods. *IEEE Transactions on Control Systems*
- 375 *Technology*, 2013, 21(4): 1207-1214.
- 376 [7] Ahmad M, Azuma S, Sugie T. A model-free approach for maximizing power production of wind farm using multi-resolution simultaneous perturbation
- 377 stochastic approximation. *Energies*, 2014, 7(9): 5624-5646.
- 378 [8] Gebraad P M O, Van Wingerden J W. Maximum power-point tracking control for wind farms. *Wind Energy*, 2015, 18(3): 429-447.
- 379 [9] Maronga B, Gryschka M, Heinze R, et al. The Parallelized Large-Eddy Simulation Model (PALM) version 4.0 for atmospheric and oceanic flows: model
- 380 formulation, recent developments, and future perspectives. *Geoscientific Model Development Discussions* 8 (2015), Nr. 2, S. 1539-1637, 2015.
- 381 [10] Park J, Law K H. Cooperative wind turbine control for maximizing wind farm power using sequential convex programming. *Energy Conversion and*
- 382 *Management*, 2015, 101: 295-316.
- 383 [11] Gebraad P M O, Teeuwisse F W, Van Wingerden J W, et al. Wind plant power optimization through yaw control using a parametric model for wake effects—
- 384 a CFD simulation study. *Wind Energy*, 2016, 19(1): 95-114.
- 385 [12] Park J, Law K H. A data-driven, cooperative wind farm control to maximize the total power production. *Applied Energy*, 2016, 165: 151-165.
- 386 [13] Park J, Law K H. Bayesian ascent: A data-driven optimization scheme for real-time control with application to wind farm power maximization. *IEEE*
- 387 *Transactions on Control Systems Technology*, 2016, 24(5): 1655-1668.
- 388 [14] Marden J R, Ruben S D, Pao L Y. A model-free approach to wind farm control using game theoretic methods. *IEEE Transactions on Control Systems*
- 389 *Technology*, 2013, 21(4): 1207-1214.
- 390 [15] Boersma S, Doekemeijer B M, Siniscalchi-Minna S, et al. A constrained wind farm controller providing secondary frequency regulation: An LES study.
- 391 *Renewable Energy*, 2019, 134: 639-652.
- 392 [16] Zhong S, Wang X. Decentralized Model-Free Wind Farm Control via Discrete Adaptive Filtering Methods. *IEEE Transactions on Smart Grid*, 2018, 9(4):
- 393 2529-2540.
- 394 [17] Munters W, Meyers J. An optimal control framework for dynamic induction control of wind farms and their interaction with the atmospheric boundary layer.
- 395 *Philosophical Transactions of the Royal Society A: Mathematical, Physical and Engineering Sciences*, 2017, 375(2091): 20160100.
- 396 [18] Quick J, Annoni J, King R, et al. Optimization under uncertainty for wake steering strategies. *Journal of Physics: Conference Series*. IOP Publishing, 2017,
- 397 854(1): 012036.
- 398 [19] Vali M, Petrović V, Boersma S, et al. Adjoint-based model predictive control for optimal energy extraction in waked wind farms. *Control Engineering Practice*,
- 399 2019, 84: 48-62.
- 400 [20] Siniscalchi-Minna S, Bianchi F D, De-Prada-Gil M, et al. A wind farm control strategy for power reserve maximization. *Renewable energy*, 2019, 131: 37-
- 401 44.
- 402 [21] Shapiro C R, Bauweraerts P, Meyers J, et al. Model-based receding horizon control of wind farms for secondary frequency regulation. *Wind Energy*, 2017,
- 403 20(7): 1261-1275.

- 404 [22] Spudić V, Conte C, Baotić M, et al. Cooperative distributed model predictive control for wind farms. *Optimal Control Applications and Methods*, 2015, 36(3):  
405 333-352.
- 406 [23] Zhao H, Wu Q, Guo Q, et al. Optimal active power control of a wind farm equipped with energy storage system based on distributed model predictive control.  
407 *IET Generation, Transmission & Distribution*, 2016, 10(3): 669-677.
- 408 [24] Jensen N O. A note on wind generator interaction. 1983.
- 409 [25] Rosolia U, Borrelli F. Learning model predictive control for iterative tasks: A computationally efficient approach for linear system. *IFAC-PapersOnLine*,  
410 2017, 50 (1): 3142-3147.
- 411 [26] Rosolia U, Borrelli F. Learning model predictive control for iterative tasks. a data-driven control framework. *IEEE Transactions on Automatic Control*, 2018,  
412 63(7): 1883-1896.
- 413 [27] Davis L. *Handbook of genetic algorithms*. 1991.
- 414 [28] Rosolia U, Borrelli F. Learning model predictive control for iterative tasks. arXiv preprint arXiv:1609.01387, 2016.
- 415 [29] Niayifar, A. and Porté-Agel, F. A new 15 analytical model for wind farm power prediction, in: *Journal of Physics: Conference Series*, vol. 625, p. 012039,  
416 IOP Publishing, 2015.
- 417 [30] Dilip, D. and Porté-Agel, F.: Wind Turbine Wake Mitigation through Blade Pitch Offset, *Energies*, 10, 757, 2017.